Fusobacterium Nucleatum Affects Cell Apoptosis by Regulating Intestinal Flora and Metabolites to Promote the Development of Colorectal Cancer

Tingting Yu
Wenzhou Medical University School of Laboratory Medicine and Life Sciences
Ling Ji
Wenzhou Medical College First Affiliated Hospital: The First Affiliated Hospital of Wenzhou Medical University
Liqin Lou
Wenzhou Medical University School of Laboratory Medicine and Life Sciences
Shiqing Ye
Wenzhou Medical University School of Laboratory Medicine and Life Sciences
Xiaoting Fang
Wenzhou Medical University School of Laboratory Medicine and Life Sciences
Feizhao Jiang
Wenzhou Medical College First Affiliated Hospital: The First Affiliated Hospital of Wenzhou Medical University
Yongliang Lou
Wenzhou Medical University School of Laboratory Medicine and Life Sciences
Xiang Li (xiangl@wmu.edu.cn)
school of lab medicine and life sciences, Wenzhou medical university https://orcid.org/0000-0001-6346-1574

Primary research

Keywords: Intestinal flora, Metabolites, Fusobacterium nucleatum, Colorectal cancer

Posted Date: September 16th, 2021

DOI: https://doi.org/10.21203/rs.3.rs-882686/v1

Version of Record: A version of this preprint was published at Frontiers in Microbiology on March 18th, 2022. See the published version at https://doi.org/10.3389/fmicb.2022.841157.

Abstract

Background/Aims:

Intestinal flora, especially *Fusobacterium nucleatum (Fn)*, can affect the development of colorectal cancer (CRC). In this study, we examined the composition of intestinal flora and metabolites in the tissues, serum and feces of CRC patients.

Materials and Methods

CRC tissues, adjacent normal colonic tissues, and fecal and serum samples were collected from CRC patients who received surgical treatment between January 2018 and January 2020. Fecal and serum samples were collected from healthy individuals for comparison. In addition, fecal samples were collected from BALB/c female mice. SW480, a human CRC cell line, was utilized for *in vitro* studies.

Results

The abundance of *Bacteroides* and propionic acid concentration were decreased. The abundance of *Lactobacillus* and lactic acid concentration were increased in CRC tissues. KEGG pathway analysis showed that *Bacteroides* and *Lactobacillus* were related to the apoptotic pathway. Additionally, lactic acid inhibited and propionic acid promoted apoptosis among SW480 CRC cells. Similar findings were noted in the feces of *Fn* gavage mice. In addition, the abundances of *Ruminococcus*, *Prevotella*, and *Sutterell* were decreased in CRC patients. The levels of leucine and isoleucine were decreased in the serum and tumor tissues of CRC patients. Aspartate, glutamate and glutathione levels were elevated in the tissues of CRC patients only. The serum glutamine, tyrosine, valine, alanine, and histidine levels were decreased significantly.

Conclusions

Fn affected the apoptosis of CRC cells and promoted the progression of CRC by affecting the distribution of intestinal flora, which altered the concentrations of metabolites such as lactic acid, propionic acid, and amino acids.

Background

Colorectal cancer (CRC) is one of the most common cancers worldwide in both sexes with more than 1.85 million new cases and 850 000 deaths every year [1, 2]. Intestinal microbes have been found to play an important role in CRC development [3–6]. The gut microbiota consists of more than 1000 species of bacteria, and the number of encoded genes within these species is 150 times that of human genes [7, 8].

Microbial colonization in known to impact glucose, amino acid and lactic acid metabolism [9]. *Lactobacillus* is one of the main intestinal floras producing lactic acid. Additionally, *Lactobacillus* participates in amino acid metabolism via a proteolytic system consisting of proteinases and peptidases to obtain amino acids [10]. Previous studies have reported that about 15% of *Lactobacillus* strains detected in fermented Asian foods produce glutamic acid [11]. *Bacteroides*, a common intestinal flora, ferments complex sugars into many by-products, including short-chain fatty acids (SCFA), such as propionate, formate, acetate and butyrate. Genome-wide association studies have shown that the proportion of *Bacteroides* in the stool of obese individuals is significantly reduced, and its proportion in stools negatively correlates with serum glutamate levels [12]. Liu *et al.* reported that depletion of species from the *Bacteroides* genus in obese individuals is related to a higher concentration of aromatic amino acids (AAA) and branched chain amino acids (BCAA) such as valine and leucine in the circulation [12].

Dysregulated cellular apoptosis plays an important role in the development of certain cancers. Bonfili *et al.* found that caspase-mediated apoptosis can be induced in HCT116 CRC cells by treatment with a mixture of essential amino acids (EAA) and non-essential amino acids (NEAA) [13]. Recent evidence suggests that *Fusobacterium nucleatum* (*Fn*) promotes the formation and development of CRC [14–16]. Zhang *et al*. showed that the abundance of *Fn* as estimated by quantitative PCR (qPCR) is significantly higher in the tumor tissues and feces samples of CRC patients [17]. In a study by Mima *et al*. involving 1069 CRC patients, the authors found that the higher abundance of *Fn* was significantly associated with shorter survival [18]. However, the exact underlying mechanisms by which *Fn* promotes tumor growth are still unknown.

In the present study, we determined the metabolites in the serum and colonic tissues of CRC patients and the composition of the bacterial flora in their feces. We also explored the impact of *Fn* on CRC by studying the fecal metabolites in mice after oral gavage of *Fn*.

Materials And Methods

Study subjects. Patients with histologically confirmed CRC who underwent surgical treatment at the First Affiliated Hospital of Wenzhou Medical University, Zhejiang, China between June 2018 and January 2020 were prospectively enrolled in this study. The study was approved by the Ethics Committee of the First Affiliated Hospital of Wenzhou Medical University. Written informed consent was obtained from all participants (patients and healthy subjects) before participation in the study.

The samples collected from the patients included resected CRC tissues, colonic tissues adjacent to the tumor, feces, and serum. Tumor staging was done according to the American Joint Committee on Cancer (AJCC), 8th edition. All fresh resected tissues and fecal samples were taken to the laboratory within 30 minutes and stored at -80°C within 2 hours. Additionally, in July 2019, 61 fecal samples from 61 healthy subjects were collected for the control group. The 61 healthy subjects, aged 40–62 years, were selected as controls during a routine physical examination in the First Affiliated Hospital of Wenzhou Medical University, and none of them had had a gastrointestinal tract disorder or taken any antibiotics in the

previous 3 months before sample collection. Total fecal DNA was obtained using an extraction kit (Hangzhou Guhe Biotechnology Co., Ltd., Hangzhou, China) according to the manufacturer's protocol. The V4 region of the bacterial 16S rDNA marker gene (16S V4) was polymerase chain reaction (PCR) amplified and sequenced by Hangzhou Guhe Biotechnology Co., Ltd.

Nuclear magnetic resonance (NMR) for metabolism.

The fresh CRC tissues were carefully dissected to obtain 200–500 mg of tissue samples and suspended in a mixture of methanol (4 ml/g of tissue) and double distilled water (0.85 ml/g of tissue). The suspension was centrifuged with 20 strokes at 800 rpm, and 50% chloroform (2 ml/g of tissue) was added, followed by repeat homogenization. The samples were centrifuged at 1,000 rpm for 30 min at 4°C. Subsequently, the samples were separated into three layers: the top water layer, the middle layer of denatured protein and the bottom lipid layer. The water layer of each specimen was separated and evaporated to dryness under a stream of nitrogen. The residue was mixed with 580 μl D_2O containing 30 μM phosphate-buffered saline (PBS; pH = 7.4) and 0.01 mg/ml sodium-3-(trimethylsilyl)-2,2,3,3-tetradeuteriopropionate (TSP) as an internal standard (δ0.0). After centrifugation at 12,000 rpm for 5 min, the supernatant was transferred to a 5-mm NMR tube for NMR spectroscopy.

About 100 mg of the fecal sample from each participant was suspended in 1 ml PBS (0.2 $mol \cdot L^{-1}$, pH = 7.0), vortexed for 3 minutes, and then ultrasonically processed for 15 minutes. These steps were repeated thrice followed by centrifugation (12 000 rpm, 15 min, 4°C), and aspiration of the supernatant. The above-mentioned steps were repeated to obtain the precipitate after centrifugation, and the two extracts were combined. The supernatant (400 μl) was taken and placed in 5-mm NMR tubes for NMR spectroscopy.

Fn strain and culture.

The *Fn* strain (ATCC 25586) used in this study was purchased from the American Type Culture Collection (Manassas, VA, USA). The *Fn* strain was cultured in Columbia blood agar supplemented with 5% defibrinated sheep blood, 5 g/ml hemin, and 1 μg/ml vitamin K1 (Sigma-Aldrich, St. Louis, MO, USA) and incubated in a 37°C anaerobic glove box with 5% CO_2, 10% H_2, and 85% N_2.

Animal experiments. Thirty-six BALB/c female mice (4–6 weeks old) were purchased for this animal study (Beijing Vital River Laboratory Animal Technology Co., Ltd.). The study involving the experimental animals was approved by the Institutional Animal Committee of Wenzhou Medical University. The mice were divided into three groups: control group, *Fn* + NaCl group, and *Fn* + azoxymethane (AOM) group, with 12, 10, and 14 mice in each group, respectively. After 1 week of acclimatization, AOM/NaCl was injected intraperitoneally once. Then the mice were given the *Fn*/NaCl by oral gavage, once a day, for 5 consecutive days. One week after *Fn* stopped intervention, mice were given a second intraperitoneal injection of AOM. One week after the second AOM injection, *Fn* was given via another intragastric intervention for 5 days. Lastly, the mice were given water and normal food until the end of the experiment

(81st day). The concentration of the intraperitoneal AOM injection was 10 mg/kg. The amount of *Fn* used was 10^8 per mouse (OD_{600nm} = 0.1).

Mass spectrometry for metabolism.

The fecal samples and tissues collected from the mice and the CRC patients were mixed with pre-cooled methanol/acetonitrile/water solution in the ratio of 2:2:1 (v/v), followed by vortex mixing, low-temperature ultrasonic processing for 30 minutes, freezing at − 24°C for 10 minutes, and then centrifugation at 14000 rpm for 20 minutes at 4°C. Later, the supernatant was extracted and dried in vacuum. Subsequently, 100 µl of acetonitrile aqueous solution (acetonitrile: water = 1:1, v/v) was added for mass spectrometry, followed by vortex mixing and centrifugation at 14000 rpm at 4°C for 15 minutes. Finally, the samples were sent with clear liquid for analysis by Shanghai Applied Protein Technology Co., Ltd. (Shanghai, China).

SW480 cell line and culture.

SW480 cell line was obtained from ATCC and cultured in Dulbecco's Modified Eagle Medium (DMEM) supplemented with 10% fetal bovine serum (FBS) (Invitrogen, Waltham, MA, USA), 100 mg/ml streptomycin (Sangon, Shanghai, China) and 100 U/ml penicillin G (Sangon) at 37°C in an incubator containing 5% CO_2.

Statistical analysis.

The R package (ropls) was used to analyze the data after normalization to the total peak intensity. Multivariate data analysis, including orthogonal partial least-squares discriminant analysis (OPLS-DA), was performed. Seven-fold cross-validation and response permutation testing was used to evaluate the robustness of the model. The variable importance in the projection (VIP) value for each variable in the OPLS-DA model was calculated to assess its contribution to the metabolite levels. Those with a VIP value > 1 were further subjected to Student's t-test at the univariate level to measure the significance for each metabolite. *P* values less than 0.05 were considered as statistically significant.

Results

Composition of the intestinal flora of the healthy subjects and CRC patients.

Fecal samples were collected from 44 patients (T group) having CRC of different stages and 61 samples from healthy individuals (N group). The relevant demographic and clinical details are presented in Table 1. The fecal samples were used for high-throughput sequencing and sequence extraction, splicing, and optimization. All samples were selected with the smallest number of sequences in the sample. By default, a 16S rRNA sequence similarity higher than 97% can be defined as an operational taxonomic unit (OTU). According to the results of OTU clustering, a Venn diagram was drawn and the numbers of common and unique OTUs between different groups were compared. As shown in Fig. 1A, there were

1569 OTUs in the N group, 1109 OTUs in the T group, and 4688 OTUs in both groups. According to the TNM stage of CRC patients, there were 1666, 223, 97, 167, 107 unique OTUs in the N, stage I, II, III, and IV groups, respectively (Fig. 1B). The rank abundance curve showed that the abundance in the N group was higher than that in the T group, and the difference in abundance between the OTUs was smaller in the N group than that in the T group (Fig. 1C). Also, the abundance of fecal flora in patients with stage II and IV CRC was similar and the smallest among those of patients with different stages of CRC, but the difference in the abundance between OTUs was the largest (Fig. 1D).

Table 1
Clinical characteristic of all individuals

	Healthy volunteers	CRC patients
n	61	48
Age (median, range)	52,40–62	60.5, 40–76
Male/female	32/29	31/17
CRC stage		
Stage Ⅰ		14
Stage Ⅱ		10
Stage Ⅲ		14
Stage Ⅳ		10

Using the unweighted Unifrac distance to perform PCoA analysis, differences between groups were found (Fig. 1E-G). ANOSIM indicated that the difference between groups was significantly greater than the difference within groups ($R = 0.385 > 0$ and $P = 0.001$; Fig. 1H). The Chao1 index showed that the richness of the communities in the sample was different between the N and T groups, and between N and the patient groups for each stage (Fig. 1I-J). However, the Shannon and Simpson indexes reflecting the diversity of the community did not differ significantly (data not shown).

The structural analysis results for the intestinal flora in the T group and N group at the phylum level are shown in Fig. 1K and 1L. In the T group, the top six phyla were *Firmicutes*, *Bacteroidetes*, *Proteobacteria*, *Actinobacteria*, *Verrucobacteria and Fusobacteria*, and their proportions were 46.68%, 29.07%, 14.29%, 7.99%, 1.18% and 0.47%, respectively, accounting for 99.69% of the total quantity of microorganisms in the sample. In the N group, the top 6 phyla were *Bacteroidetes*, *Firmicutes*, *Proteobacteria*, *Actinobacteria*, *Fusobacteria* and *Verrucomicrobia*, and their proportions were 53.84%, 40.41%, 4.97%, 0.56%, 0.13% and 0.03%, respectively, accounting for 99.94% of the total microorganisms in the sample. At the phylum level, the relative abundances of *Bacteroidetes*, *Proteobacteria*, and *Actinobacteria* were significantly different between healthy subjects and CRC patients ($P < 0.05$).

Intestinal flora regulates cell apoptosis by affecting metabolism.

The abundance of bacteria involved in the metabolism of amino acids such as tyrosine metabolism, lysine, valine, leucine, and isoleucine was increased in the T group (Fig. 3A-D). Based on the PICRUSt function prediction of the 16S rDNA sequence, differences in the abundances in functional genes of KEGG pathways at different levels (1 ~ 3) were observed between the T group and N group. Based on this, a heat map was made at the genus level to examine the role of the genera in the different KEGG pathways. Among them, *Prevotella* and *[Ruminococcus]* were found to be involved in amino acid and tyrosine metabolism (Fig. 2). Additionally, *Prevotella* played an important role in lysine, valine, leucine, and isoleucine degradation (Fig. 2). In the stool sequencing of the T group, we found that the content of *Prevotella* was decreased and that of *[Ruminococcus]* was increased compared with the contents for the N group (Fig. 3E, F). In addition, *Bacteroides* and *Sutterel* were found to play roles in the biosynthesis of unsaturated fatty acids, fatty acid metabolism, glutathione metabolism, and lysine, valine, leucine and isoleucine degradation (Fig. 2). Notably, *Bacteroides*, *Sutterel* and *Lactobacillus* were all related to the apoptotic pathway. Also, the abundances of *Bacteroides* and *Sutterel* were decreased in the T group, while the abundance of *Lactobacillus* was increased in the T group (Fig. 2,3G-I).

We also collected cancer tissues and adjacent normal colonic tissues from 5 CRC patients, and serum samples from 4 CRC patients and 4 healthy subjects for NMR detection. In the principal component analysis scoring chart (PCOA), we saw a separation trend between the serum of T and N groups, as well as a separation trend between the cancer tissues, the adjacent colonic tissues, and the normal tissues of the CRC patients (Fig. 4A,B). Lactic acid as the main metabolite of *Lactobacillus* was found to be increased in both the serum and tumor tissues (Fig. 4C,D). The results of mass spectrometry of tumor tissues from CRC patients showed that the content of propionic acid, the main metabolite of *Bacteroides*, was also increased (Fig. 4E). Interestingly, *Lactobacillus* and *Bacteroides* had increased abundances in the feces of CRC patients relative to controls (Fig. 4G,I). In addition, the levels of leucine and isoleucine in tumor tissues were significantly lower than those in the adjacent colonic tissues. Correspondingly, the levels of leucine and isoleucine in the serum of CRC patients were lower than those in healthy subjects (Fig. 4F,G,K,L). Also, the level of lysine in CRC tissues was decreased (Fig. 4H), while the serum levels of valine, histidine, alanine and tyrosine in the CRC patients were significantly decreased (Fig. 4N-P, Supplementary Fig. 1C). Notably, the glutamine content in the serum of CRC patients was decreased, while that in the tumor tissues was increased (Fig. 4J,M). In addition, the results showed that the levels of aspartic acid and glutathione in CRC tissues were increased (Fig. 4I, Supplementary Fig. 1A).

Based on the above results, we believe that the intestinal flora plays an important role in the regulation of cell apoptosis by affecting amino acid and lactic acid metabolism.

Fn affects cell apoptosis by regulating intestinal flora and associated metabolites .

To explore the effect of oral gavage with *Fn* on the intestinal flora and the intestinal metabolites of mice, we collected feces of a control (Con) group and a *Fn* group of mice for 16S rDNA sequencing and mass spectrometry detection. The correlation analysis of the microbes at the phylum level showed that the abundance of *Fusobacteria* was positively correlated with the abundance of *Gemmatimonadetes* and

negatively correlated with the abundance of *Euryarchaeota* and *Tenericutes* (Fig. 5A). *Firmicutes* and *Bacteroidetes* were more abundant in the feces. *Firmicutes* was positively correlated with *Planctomycetes* and *Gemmatimonadetes*, but negatively correlated with *Verrucomicrobia*. Additionally, *Bacteroidetes* was positively correlated with *Actinobacteria* and *Armatimonadetes* (Fig. 5A). We used GraPhlan combined with OTU tables to display the results of OTU species annotations of all samples (Fig. 5B). Bacteria were mainly distributed in *Firmicutes*, *Bacteroidetes*, and *Proteobacteria*. For *Firmicutes*, the flora of *Ruminococcaceae* and *Lactobacillaceae* were mainly distributed in the *Fn* group. The flora of *Lachnospiraceae*, *Dehalobacteriaceae* and *Staphylococcaceae* were mainly distributed in the Con group. For *Bacteroidetes*, the flora of *Odoribacteraceae*, *Bacteroidaceae*, *Prevotellaceae*, *Paraprevotellaceae*, and *Porphyromonadaceae* were mainly distributed in the *Fn* group, and *Rikenellaceae* was mainly distributed in the Con group. The random forest algorithm was used to draw a point map of species importance, and the results showed that *Odoribacter*, *Anaerostipes*, *Lactobacillus*, *Dorea*, *Proteus*, *Prevotella*, *Roseburia* and *Ruminococcus* played major roles in the grouping effect (Fig. 5C). The comparison of phenotypic classification based on BugBase showed that the *Fn* + AOM group had the least anaerobic bacteria, and the *Fn* + AOM group and *Fn* group had higher facultative bacteria contents than the Con group (Fig. 6A,B). At the same time, in the *Fn* + AOM group and *Fn* group, the abundance of potentially pathogenic bacteria was increased (Fig. 6C). In addition, the ability for biofilm formation improved gradually in the Con, *Fn* + AOM, and *Fn* groups (Fig. 6D).

The results of KEGG pathway analysis showed that the abundance of the flora associated with the apoptosis pathway was increased in the *Fn* group (Fig. 6E). Compared with the Con group, the flora related to the MAPK signaling pathway was enriched in the *Fn* group, but decreased in the *Fn* + AOM group, which was similar to the distribution of the cytochrome p450-related flora (Fig. 6F,G). These series of results seem to point to an apoptotic pathway related to mitochondria. The analysis of the abundance of fecal flora showed that compared with the Con group, the abundance of *Odoribacter*, *Dorea*, and *Rummococcus* were increased in the Fn group but decreased in the *Fn* + AOM group. *Prevotella* increased significantly in the Fn group compared to the other two groups (Fig. 6I,L). In addition, the comparative analysis of *Fn* group and Con group showed that the abundance of *Lactobacillus* was increased significantly in the *Fn* group, but no difference was found in the three-group comparative analysis of the *Fn* group, Con group and *Fn* + AOM group (data not shown; Fig. 6H). At the same time, the correlation heat map of KEGG pathways and flora showed that *Lactobacillus*, *Odoribacter* and *Bacteroides* were related to the apoptosis pathway in the two-group comparative analysis of the *Fn* group and Con group (Fig. 7A). The above results showed that *Lactobacillus* and *Bacteroides* play an important role in the composition of the intestinal flora of mice given *Fn* gavage. OPLS-DA indicated that the model was stable (Fig. 7B). VIP > 1 and *P* value < 0.05 obtained using the OPLS-DA model were the screening criteria used to label the difference in the metabolites as significant. As shown in Fig. 7C, in the *Fn* group, 3-phenylpropanoic acid, 5-hydroxyindoleacetic acid and deoxyguanosine were decreased. However, alpha-tocopherol (vitamin E) was increased (Fig. 7C). D-lactic acid, the main metabolite of *Lactobacillus*, was significantly increased in the *Fn* group (Fig. 7C). In addition, propionic acid showed a downtrend in the *Fn* group compared to the Con group (Fig. 7D).

Based on the above results, we believe that in mice given *Fn* gavage, *Bacteroides* and *Lactobacillus* in the intestinal flora can affect cell apoptosis by regulating lactic acid and propionic acid metabolism.

Effects of lactic acid and propionic acid on the apoptosis of SW480 CRC cells.

To confirm the influence of propionic acid on the apoptosis pathway at the cellular level, we treated SW480 CRC cells with propionic acid to detect the expression of related proteins in the apoptosis pathway. We cultured SW480 cells with 15,25 mM lactic acid in a sugar-free environment for 48 hours. Western Blot analysis showed that the expression of anti-apoptotic protein Bcl-2 was increased (Fig. 8A). After treating SW480 cells with different concentrations of propionic acid, western blot analysis showed that Bax, cleaved-Parp and cleaved-caspase 3 expression increased significantly after treating the cells with 25 mM propionic acid for 48 hours. There was an upward trend in protein expression after treatment with 5 mM propionic acid, but the difference was not statistically significant (Fig. 8B). Based on these findings, we concluded that lactic acid, a metabolite of *Lactobacillus*, inhibited the apoptosis of SW480 cells, while propionic acid, a metabolite of *Bacteroides*, promoted apoptosis among SW480 cells.

Discussion

The results of this study indicate that the intestinal flora plays an important role in the occurrence and progression of CRC. We found that the abundance and diversity of the flora are decreased in the feces of CRC patients, which is consistent with previous results (Fig. 1). In addition, *Fusobacterium* was found to be associated with the apoptotic pathway (Fig. 2). These findings indicated that *Fn* could play an important role in the occurrence and development of CRC. We have confirmed in our previous work that at the cellular level, *Fn* promotes the progression of CRC through the Cdk5-activated Wnt/β-catenin signaling [19]. The experiments of the present study showed that the intestinal flora of mice given *Fn* gavage mainly included *Firmicutes*, *Bacteroidetes*, and *Proteobacteria* (Fig. 5B). In addition, the abundances of *Lactobacillaceae*, *Odoribacteraceae*, *Bacteroidaceae*, *Prevotellaceae*, and *Paraprevotellaceae* were increased in the *Fn* group (Fig. 5B). At the same time, certain bacterial genera in these families such as *Lactobacillus*, *Bacteroides*, *Odoribacter*, and *Parabacteroides* were related to the apoptosis pathway, and the abundances of *Lactobacillus* and *Odoribacter* were increased in the *Fn* group (Fig. 6H, 6I, 7A). The KEGG pathway analysis showed that the abundance of anaerobic, facultative and potentially pathogenic bacteria was increased in the *Fn* group (Fig. 6A-C). The capability for biofilm formation improved gradually in the Con, *Fn* + AOM, and *Fn* groups (Fig. 6D). The results indicated that *Fn* could regulate the composition and related functions of the intestinal flora to promote the development of CRC.

Jacobson *et al.* found that propionate produced by *Bacteroides* directly inhibits *Salmonella enterica serovar Typhimurium* growth *in vitro* by disrupting intracellular pH homeostasis and also limits their fecal shedding *in vivo* [20]. We observed a downward trend in the propionic acid level in cancer tissues of CRC patients, and the abundance of propionic acid-producing *Bacteroides* was decreased significantly (Fig.s 3G,4E). The KEGG pathway analysis showed that *Bacteroides* were related to the apoptotic pathway (Fig. 2). The same findings were noted in the stool of mice given *Fn* gavage. In *these* mice, the KEGG

pathway analysis of propionic acid-producing *Bacteroides* was found to be related to the apoptosis pathway (Fig. 7A). The content of propionic acid was decreased in the feces of mice given *Fn* gavage but not statistically significant due to the limited number of mice (Fig. 7D). We also found that propionic acid promoted the apoptosis of SW480 CRC cells (Fig. 8B).

Chan e*t al.* found that the content of lactic acid was increased in cancer tissues with the tissue metabolism profile [21]. In our study, we also found that the content of lactic acid in the serum and cancer tissues of CRC patients was increased (Fig. 4C,D), and the abundance of lactic acid-producing *Lactobacillus* was increased significantly. The KEGG pathway analysis showed that *Lactobacillus* was related to the apoptotic pathway (Fig. 2, 3I). Similarly, the KEGG pathway analysis of lactic acid-producing *Lactobacillus* was also found to be related to the apoptosis pathway in mice given *Fn* gavage (Fig. 7A,C). It is worth noting that when compared with that in the control group, the abundance of *Lactobacillus* in the *Fn* group was significantly increased ($P < 0.05$). When the *Fn*, *Fn* + AOM and control groups were compared, no statistical difference was found in the distribution of *Lactobacillus* (data not shown; Fig. 6H). The in vitro experiment in this study found that lactic acid inhibited the apoptosis of SW480 cells (Fig. 8A).

In addition, the intestinal flora related to the MAPK and cytochrome p450 pathways were enriched in the *Fn* group. Among them, *Odoribacter* and *Rummoccus* were related to the MAPK pathway, while *Bacteroides* was related to the cytochrome p450 pathway (Supplementary Fig. 1A, Fig. 6I,L). The mammalian p450s are all membrane-bound (mostly bound to the endoplasmic reticulum, but some to mitochondria) [22]. The MAPK pathway plays an important role in regulating apoptosis related to growth factors in CRC [23]. Whether *Fn* regulates mitochondrial function by regulating the MAPK signaling pathways and cytochrome p450 and then affects cell apoptosis remains to be explored.

We believe that *Fn* promotes the progression of CRC by affecting the distribution of *Bacteroides* and *Lactobacillus*. *Bacteroides* and *Lactobacillus* can affect the apoptosis of CRC cells through metabolites such as lactic acid, propionic acid and amino acids. In a study by Li *et al.* involving the serum samples of 120 healthy volunteers, 120 multiple sclerosis patients, and 120 age- and gender-matched CRC patients, the contents of tyrosine and Glu-Leu dipeptide were decreased in CRC patients, which indicated that the combination of Glu-Leu and tyrosine in serum might be useful as a new biomarker for the early diagnosis of CRC [24]. Similarly, in the current study, the serum tyrosine levels of CRC patients were significantly decreased (Fig. 4O). These findings might be due to higher utilization of the amino acids by CRC cells to maintain the rapid cell proliferation [25]. Also, research has shown that hypoxia-responsive miRNAs might be involved in the targeted regulation of β-alanine, valine, leucine, and isoleucine metabolism [26]. Our results showed that alanine and valine were decreased in serum of CRC patients (Fig. 4N,P). Also, leucine and isoleucine were decreased in serum and tissues of CRC patients (Fig. 4F,G,K,L). Whether the intestinal flora regulates the amino acid metabolism through hypoxia-responsive miRNA remains to be studied. The results showed that the content of glutathione in CRC tissues was increased (Fig. 4I). Excessive glutathione has been reported to be associated with tumor progression and distant metastasis [27]. In this study, we found that *Bacteroides*, *Prevotella*, and *Sutterella* played important roles in glutathione

metabolism (Fig. 2). However, it was interesting that the relative abundance of these three genera in the feces of T group decreased (Fig. 3E,G,H). Experiments have also shown that bacteria used histidine to produce histamine and to prevent the translocation of intestinal bacteria [25]. In our results, the serum histidine levels in the CRC patients were significantly decreased, which might be due to the decrease in the absorption of histidine into the blood circulation by intestinal flora (Supplementary Fig. 1B). Studies had also found that the level of aspartic acid in cancer tissues of the stomach and colon was significantly higher than that in the normal full-thickness or mucosal layer [28]. This was consistent with our results. The aspartic acid level in CRC tissues was significantly higher than that in the adjacent colonic tissues (Supplementary Fig. 1C).

Conclusion

Fn promoted the progression of CRC by affecting the distribution of intestinal flora. Intestinal flora affected the apoptosis of CRC cells through metabolites such as lactic acid, propionic acid, and amino acids. Hence, it is important to explore the role of intestinal flora and their metabolites in the occurrence and development of CRC. This may help to find more effective newer therapeutic targets for treating CRC.

Declarations

Authors' contributions

Study concept and design: LX, LYL; Specimen collection: JL, JFZ; Analysis and interpretation of data and statistical analysis: YTT, YSQ, FXT, LLQ; Animal experiments:, YTT, FXT, YSQ; Drafting the manuscript: LX, LYL.

Acknowledgements

Not applicable.

Competing interests

The authors declare that they have no competing interests.

Availability of data and materials

The datasets used and/or analyzed during the current study are available from the corresponding author on reasonable request.

Consent for publication

Not applicable.

Ethics approval and consent to participate

The study was approved by the Ethics Committee of the First Affiliated Hospital of Wenzhou Medical University(Wenzhou, China).

Funding

This work was supported by grants from National Science and Technology Major Project (No. 2018ZX10201001), the Key Discipline of Zhejiang Province in Medical Technology (First Class, Category A), Health Project of the Science and Technology Department of Wenzhou (No.Y20180070) andthe Zhejiang Province Science and Technology Plan Research and Xinmiao Talent Program (Grant No. 2020R413078).

Publisher's Note

References

1. Torre LA, Bray F, Siegel RL, Ferlay J, Lortet-Tieulent J, Jemal A: Global cancer statistics, 2012. *CA: a cancer journal for clinicians* 2015, 65(2):87-108.
2. Biller LH, Schrag D: Diagnosis and Treatment of Metastatic Colorectal Cancer: A Review. *Jama* 2021, 325(7):669-685.
3. Rowland IR: The role of the gastrointestinal microbiota in colorectal cancer. *Curr Pharm Des* 2009, 15(13):1524-1527.
4. Wang T, Cai G, Qiu Y, Fei N, Zhang M, Pang X, Jia W, Cai S, Zhao L: Structural segregation of gut microbiota between colorectal cancer patients and healthy volunteers. *Isme j* 2012, 6(2):320-329.
5. Zhu Q, Gao R, Wu W, Qin H: The role of gut microbiota in the pathogenesis of colorectal cancer. *Tumour Biol* 2013, 34(3):1285-1300.
6. Wang Y, Zhang X, Li J, Zhang Y, Guo Y, Chang Q, Chen L, Wang Y, Wang S, Song Y *et al*: Sini Decoction Ameliorates Colorectal Cancer and Modulates the Composition of Gut Microbiota in Mice. *Front Pharmacol* 2021, 12:609992.
7. Qin J, Li R, Raes J, Arumugam M, Burgdorf KS, Manichanh C, Nielsen T, Pons N, Levenez F, Yamada T *et al*: A human gut microbial gene catalogue established by metagenomic sequencing. *Nature* 2010, 464(7285):59-65.
8. Zou S, Fang L, Lee MH: Dysbiosis of gut microbiota in promoting the development of colorectal cancer. *Gastroenterol Rep (Oxf)* 2018, 6(1):1-12.
9. Zhou CB, Fang JY: The regulation of host cellular and gut microbial metabolism in the development and prevention of colorectal cancer. *Crit Rev Microbiol* 2018, 44(4):436-454.
10. Law BA, Kolstad J: Proteolytic systems in lactic acid bacteria. *Antonie Van Leeuwenhoek* 1983, 49(3):225-245.

11. Zareian M, Ebrahimpour A, Bakar FA, Mohamed AK, Forghani B, Ab-Kadir MS, Saari N: A glutamic acid-producing lactic acid bacteria isolated from Malaysian fermented foods. *Int J Mol Sci* 2012, 13(5):5482-5497.
12. Liu R, Hong J, Xu X, Feng Q, Zhang D, Gu Y, Shi J, Zhao S, Liu W, Wang X *et al*: Gut microbiome and serum metabolome alterations in obesity and after weight-loss intervention. *Nat Med* 2017, 23(7):859-868.
13. Bonfili L, Cecarini V, Cuccioloni M, Angeletti M, Flati V, Corsetti G, Pasini E, Dioguardi FS, Eleuteri AM: Essential amino acid mixtures drive cancer cells to apoptosis through proteasome inhibition and autophagy activation. *Febs j* 2017, 284(11):1726-1737.
14. Kostic AD, Chun E, Robertson L, Glickman JN, Gallini CA, Michaud M, Clancy TE, Chung DC, Lochhead P, Hold GL *et al*: Fusobacterium nucleatum potentiates intestinal tumorigenesis and modulates the tumor-immune microenvironment. *Cell Host Microbe* 2013, 14(2):207-215.
15. Gur C, Ibrahim Y, Isaacson B, Yamin R, Abed J, Gamliel M, Enk J, Bar-On Y, Stanietsky-Kaynan N, Coppenhagen-Glazer S *et al*: Binding of the Fap2 protein of Fusobacterium nucleatum to human inhibitory receptor TIGIT protects tumors from immune cell attack. *Immunity* 2015, 42(2):344-355.
16. Yang Y, Weng W, Peng J, Hong L, Yang L, Toiyama Y, Gao R, Liu M, Yin M, Pan C *et al*: Fusobacterium nucleatum Increases Proliferation of Colorectal Cancer Cells and Tumor Development in Mice by Activating Toll-Like Receptor 4 Signaling to Nuclear Factor-κB, and Up-regulating Expression of MicroRNA-21. *Gastroenterology* 2017, 152(4):851-866.e824.
17. Zhang X, Zhu X, Cao Y, Fang JY, Hong J, Chen H: Fecal Fusobacterium nucleatum for the diagnosis of colorectal tumor: A systematic review and meta-analysis. *Cancer Med* 2019, 8(2):480-491.
18. Mima K, Nishihara R, Qian ZR, Cao Y, Sukawa Y, Nowak JA, Yang J, Dou R, Masugi Y, Song M *et al*: Fusobacterium nucleatum in colorectal carcinoma tissue and patient prognosis. *Gut* 2016, 65(12):1973-1980.
19. Li X, Huang J, Yu T, Fang X, Lou L, Xin S, Ji L, Jiang F, Lou Y: Fusobacterium nucleatum Promotes the Progression of Colorectal Cancer Through Cdk5-Activated Wnt/β-Catenin Signaling. *Front Microbiol* 2020, 11:545251.
20. Jacobson A, Lam L, Rajendram M, Tamburini F, Honeycutt J, Pham T, Van Treuren W, Pruss K, Stabler SR, Lugo K *et al*: A Gut Commensal-Produced Metabolite Mediates Colonization Resistance to Salmonella Infection. *Cell Host Microbe* 2018, 24(2):296-307.e297.
21. Chan EC, Koh PK, Mal M, Cheah PY, Eu KW, Backshall A, Cavill R, Nicholson JK, Keun HC: Metabolic profiling of human colorectal cancer using high-resolution magic angle spinning nuclear magnetic resonance (HR-MAS NMR) spectroscopy and gas chromatography mass spectrometry (GC/MS). *J Proteome Res* 2009, 8(1):352-361.
22. Guengerich FP: Cytochrome P450 research and The Journal of Biological Chemistry. *J Biol Chem* 2019, 294(5):1671-1680.
23. Fang JY, Richardson BC: The MAPK signalling pathways and colorectal cancer. *Lancet Oncol* 2005, 6(5):322-327.

24. Li J, Li J, Wang H, Qi LW, Zhu Y, Lai M: Tyrosine and Glutamine-Leucine Are Metabolic Markers of Early-Stage Colorectal Cancers. *Gastroenterology* 2019, 157(1):257-259.e255.
25. Snell K, Natsumeda Y, Eble JN, Glover JL, Weber G: Enzymic imbalance in serine metabolism in human colon carcinoma and rat sarcoma. *Br J Cancer* 1988, 57(1):87-90.
26. Nijhuis A, Thompson H, Adam J, Parker A, Gammon L, Lewis A, Bundy JG, Soga T, Jalaly A, Propper D *et al*: Remodelling of microRNAs in colorectal cancer by hypoxia alters metabolism profiles and 5-fluorouracil resistance. *Hum Mol Genet* 2017, 26(8):1552-1564.
27. Bansal A, Simon MC: Glutathione metabolism in cancer progression and treatment resistance. *J Cell Biol* 2018, 217(7):2291-2298.
28. Okada A, Takehara H, Yoshida K, Nishi M, Miyake H, Kita Y, Komi N: Increased aspartate and glutamate levels in both gastric and colon cancer tissues. *Tokushima J Exp Med* 1993, 40(1-2):19-25.

Figures

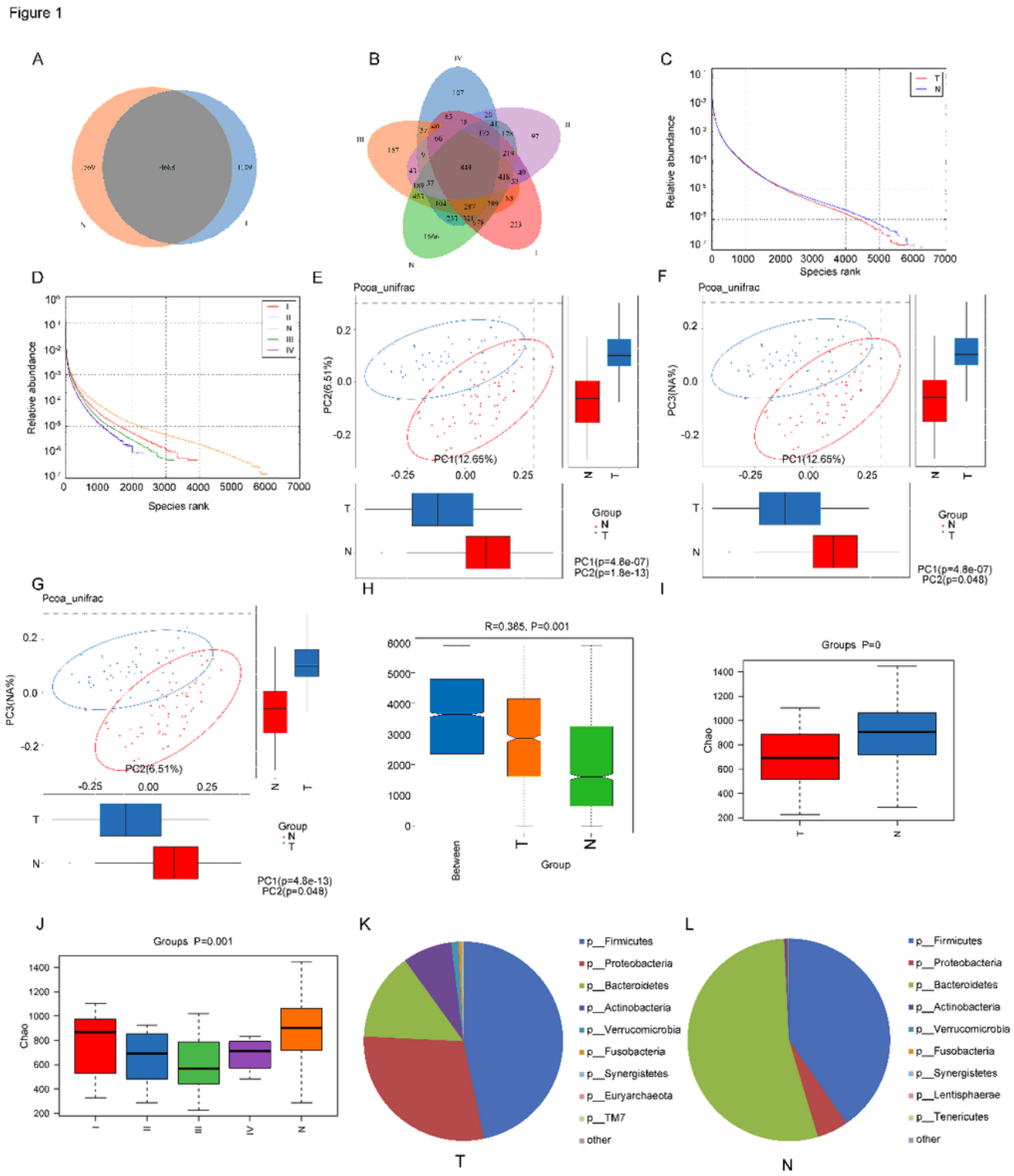

Figure 1

Comparison of the composition of intestinal flora between healthy subjects and CRC patients. (A, B): Venn diagrams according to the different grouping methods; (C, D): rank abundance curve according to the different grouping methods; (E-G): principal Co-ordinates Analysis (PCoA) with unweighted Unifrac distance; (H): use of ANOSIM to analyze differences between the groups and within the groups; (I,J):

Chao1 index analysis according to the different grouping methods; and K,L: analysis of the composition of the intestinal flora of cancer patients and healthy subjects at the phylum level.

Figure 2

Correlation analysis heat map of bacteria and KEGG pathways.

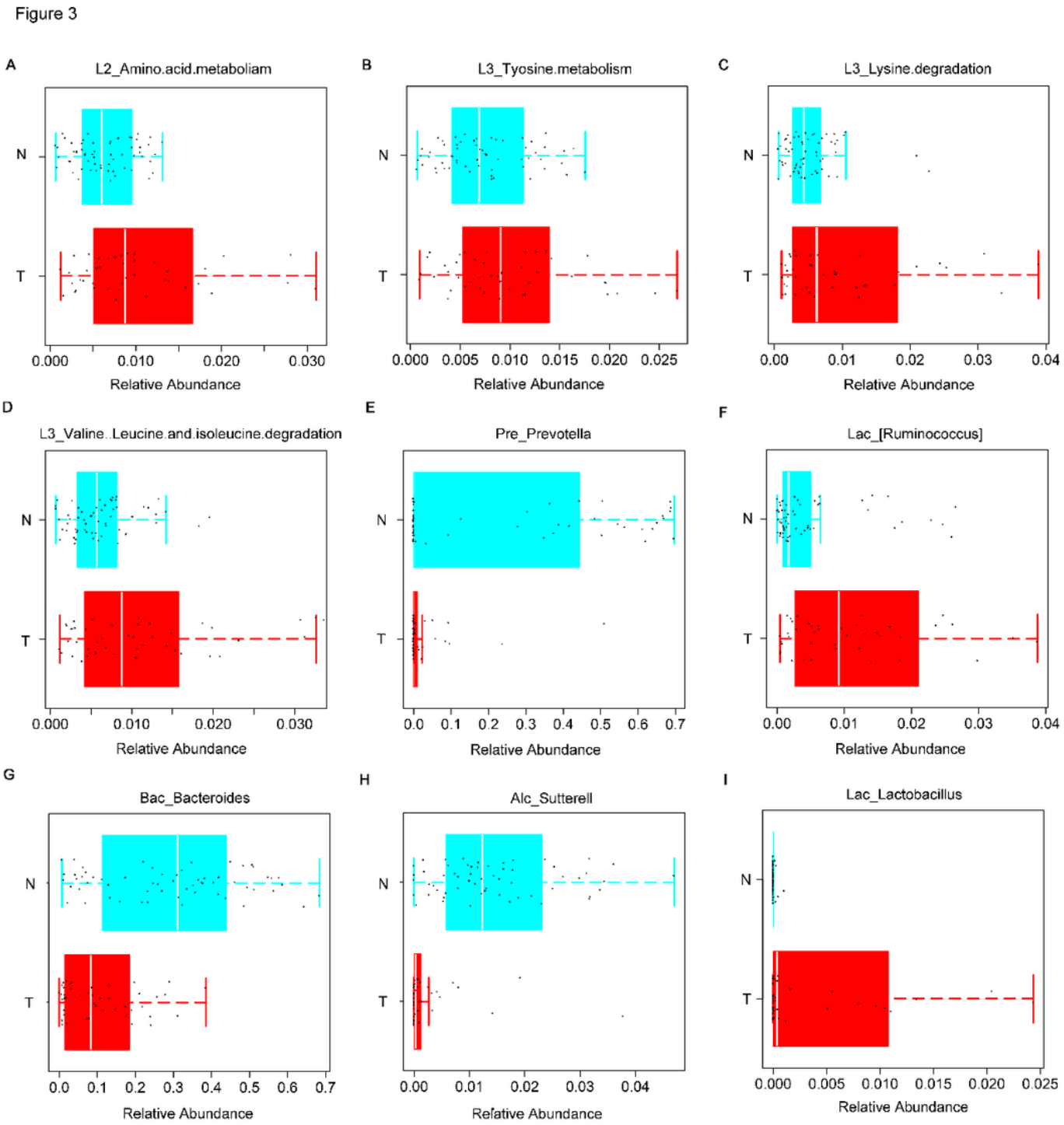

Figure 3

KEGG functions and related bacteria in the CRC group (T) and healthy group (N).(A-D):The relative abundances of genera related to different KEGG functions in T and N groups; (E-I): bacteria with statistical difference between the T and N groups.

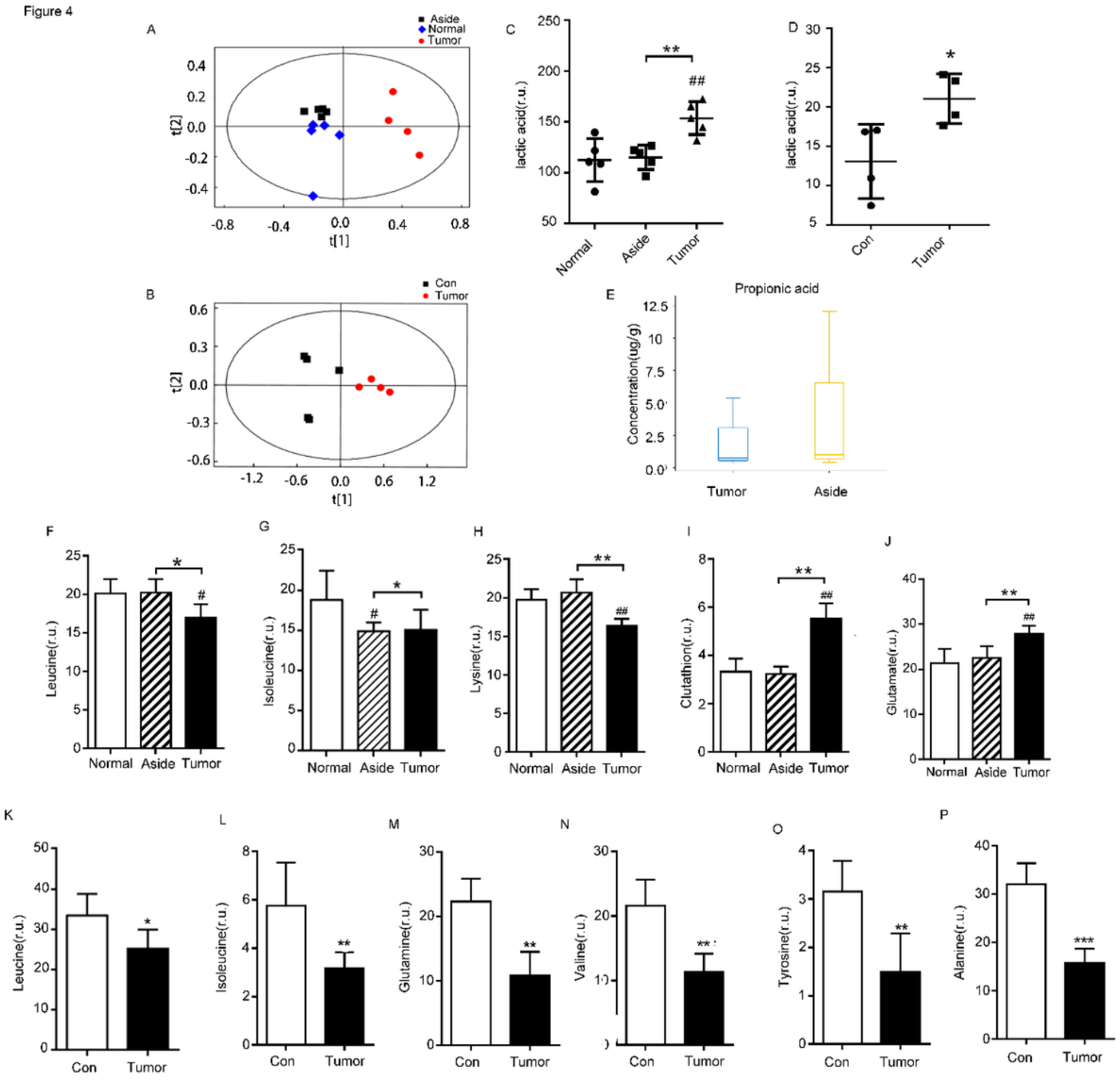

Figure 4

Detection of metabolites in the tissues and serum of CRC patients and healthy people. (A,B):Principal component analysis (PCA) of metabolites in tissues and serum of CRC patients, respectively; (C,D): detection of lactic acid in tissues and serum of CRC patients, respectively; (E): propionic acid in tissues of CRC patients; (F-J): differential metabolites in various tissues of CRC patients with NMR, #P<0.05, ##P<0.01, *P<0.05, **P<0.01; and K-P: differential metabolites in serum of CRC patients and healthy individuals, *P<0.05, **P<0.01, ***P<0.001.

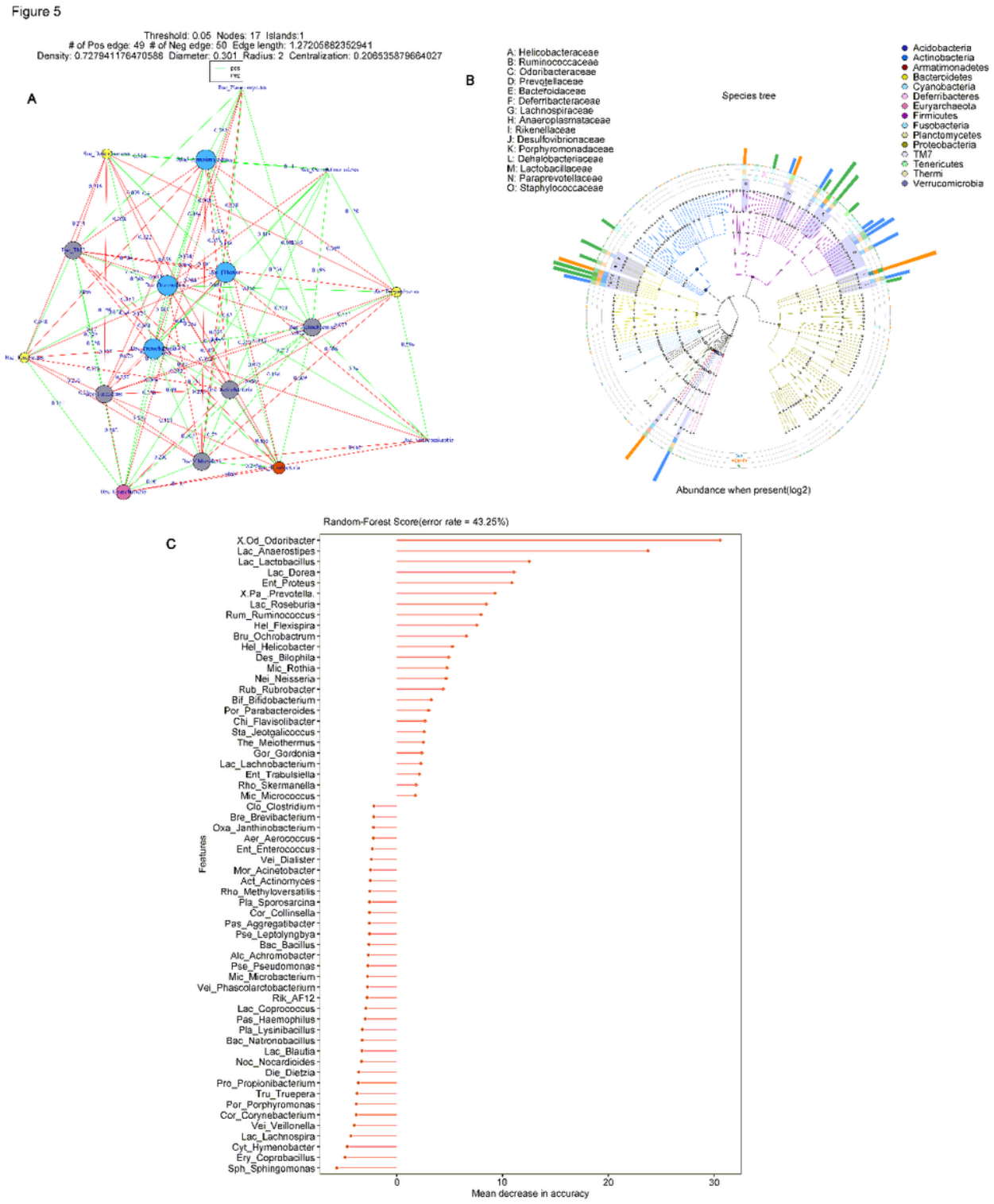

Figure 5

Sequencing analysis of the fecal samples from mice given Fn gavage. (A): The relationship between microorganisms at the phylum level; (B): distribution map of sample community of species evolutionary tree; and C: species importance point map.

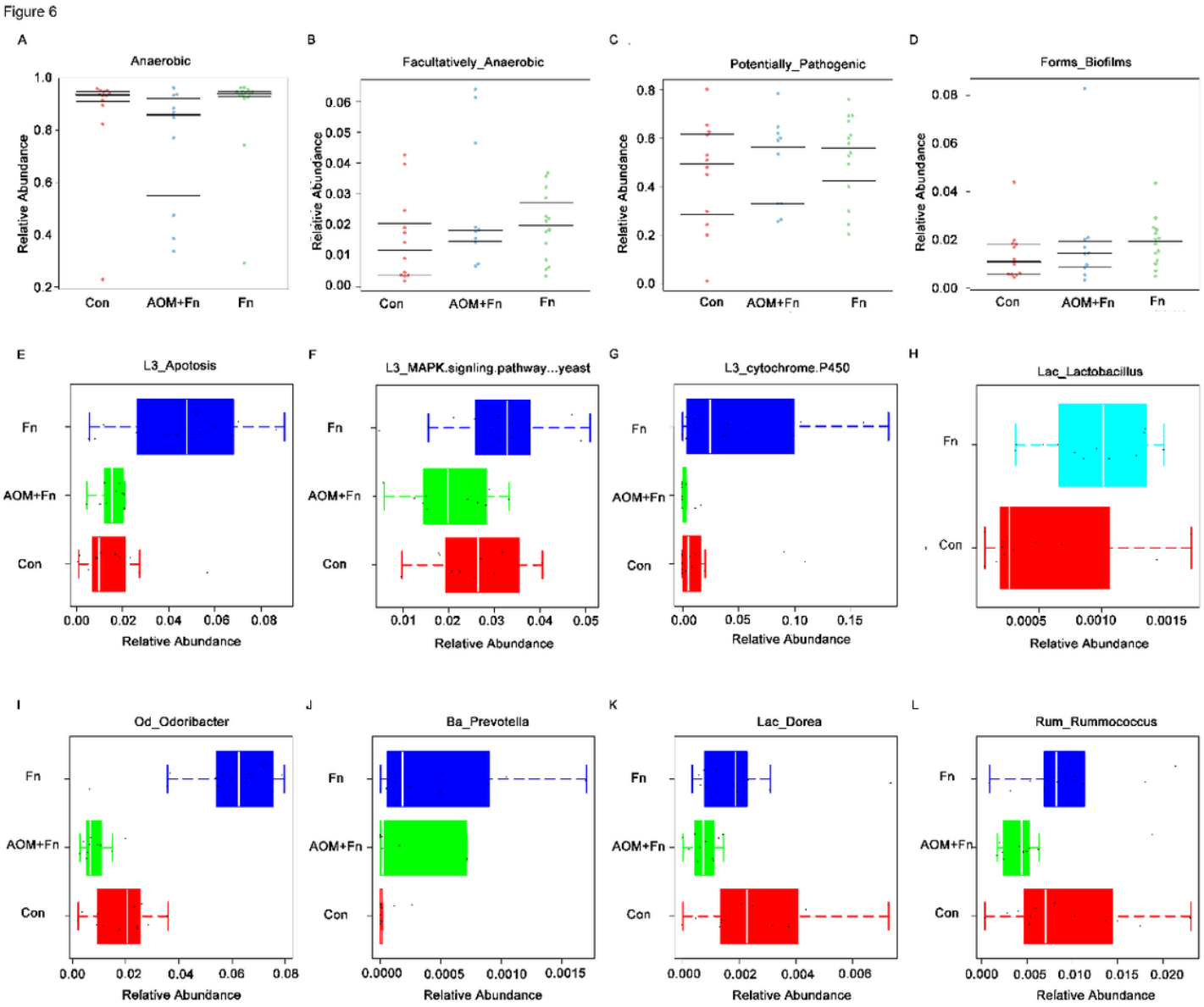

Figure 6

Sequencing analysis of the fecal samples from mice given Fn gavage. (A-G): The relative abundances of genera related to different KEGG functions in the Fn group and control group; (H): distribution of Lactobacillus in the Fn group and control group; (I-L): bacteria with statistical difference in expression between the Fn group, Fn+AOM group and control group.

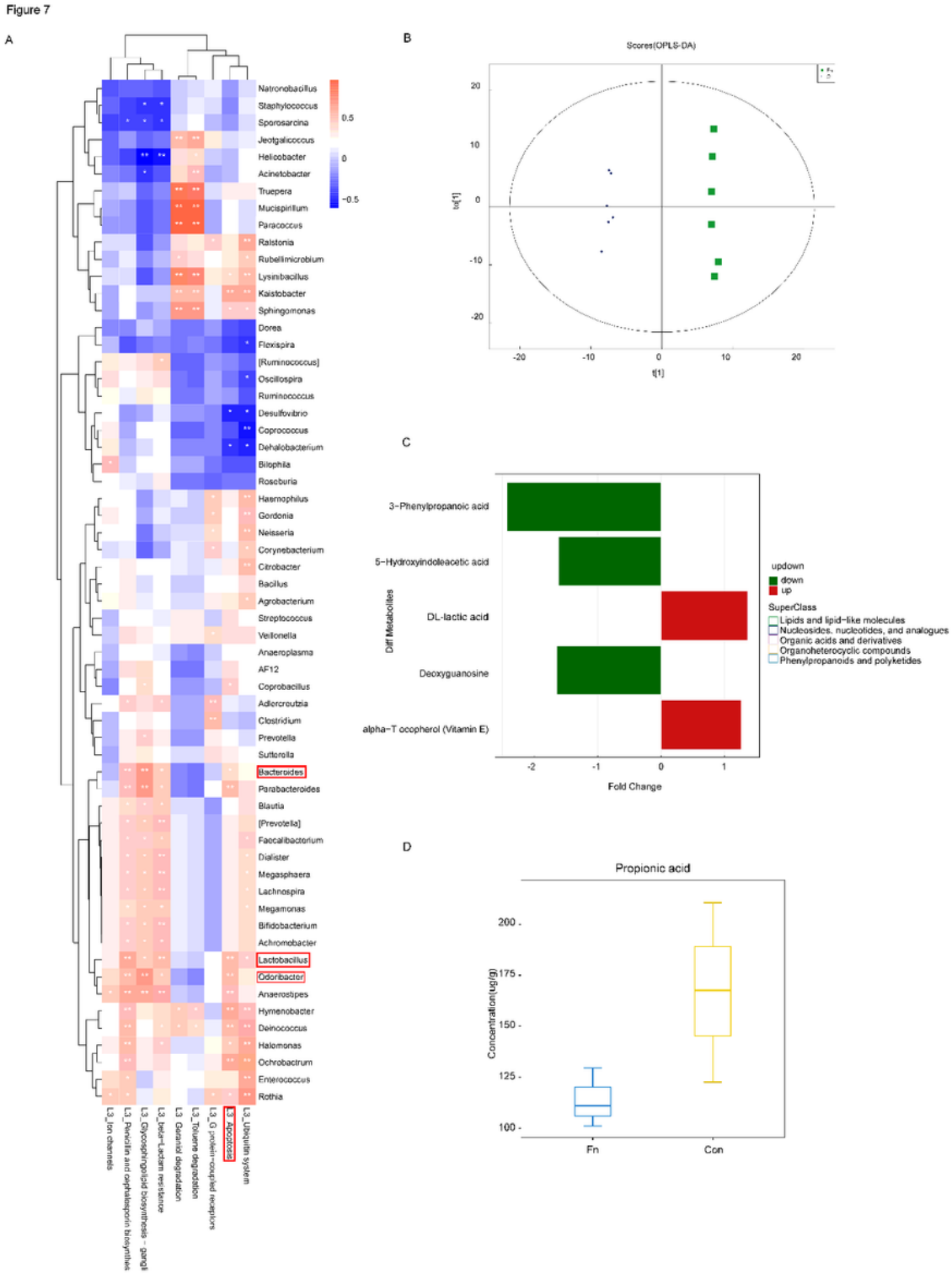

Figure 7

KEGG pathway and metabolite analysis of the fecal samples from mice given Fn gavage. (A): Correlation analysis heat map of bacteria and KEGG pathways in Con and Fn groups. (B): OPLS-DA showed the stability of the template; (C): differential metabolites identified with non-targeted mass spectrometry; (D): propionic acid identified with targeted mass spectrometry.

Figure 8

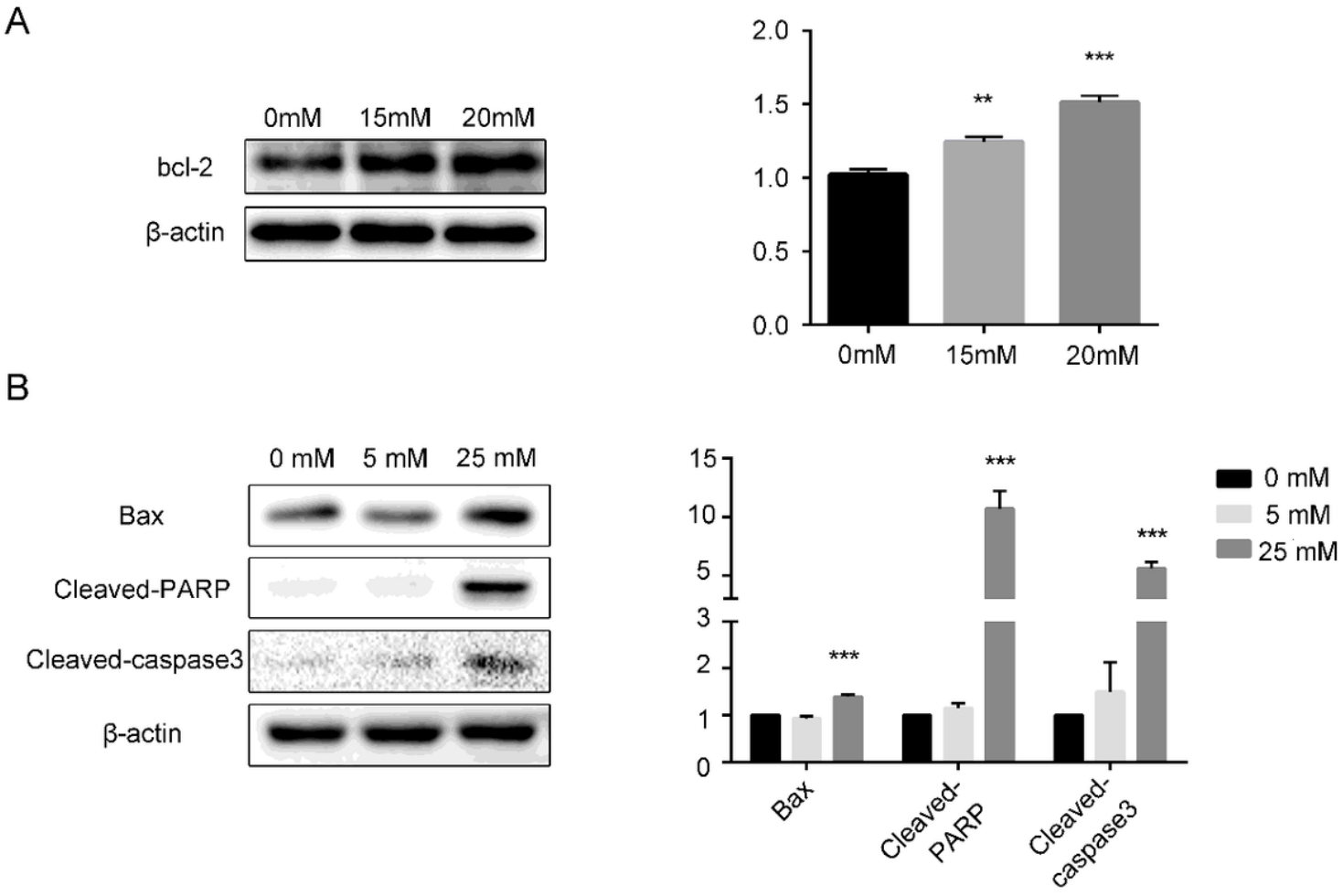

Figure 8

The influence of lactic acid and propionic acid on the apoptosis of SW480 cells. (A): Lactic acid inhibited the apoptosis of SW480 colorectal cancer cells. (B): Propionic acid promoted the apoptosis of the SW480 colorectal cancer cells. ***P<0.001 vs. control

Supplementary Files

This is a list of supplementary files associated with this preprint. Click to download.

- Onlinefloatimage9.png